Applied Nanoscience (2022) 12:835–848
https://doi.org/10.1007/s13204-021-01749-z

REVIEW ARTICLE

Preparation and characterization of nanocellulose obtained by TEMPO-mediated oxidation of organosolv pulp from reed stalks

V. A. Barbash[1] · O. V. Yashchenko[1] · A. S. Gondovska[1] · I. M. Deykun[1]

Received: 29 December 2020 / Accepted: 12 February 2021 / Published online: 7 March 2021

Abstract

Renewable plant materials are of interest for the development of new biodegradable materials. The study describes the preparation process of nanocellulose from organosolv reed pulp (ORP). ORP was obtained from reed stalks in two stages: by extraction of the raw material with NaOH solution and cooking using a mixture of acetic acid and hydrogen peroxide. Nanocellulose was extracted from ORP using 2,2,6,6-tetramethylpiperidine-1-oxyl (TEMPO) in a TEMPO/NaBr/NaClO system followed by ultrasonic treatment to obtain a stable nanocellulose gel. It was found that an increase in the TEMPO consumption and oxidation time increases the density and tensile strength, the content of carboxyl groups, and the transparency of the nanocellulose films, but decreases the yield and crystallinity of the nanocellulose. Structural and chemical changes and the crystallinity index of reed stalks, ORP, and nanocellulose were studied using SEM, FTIR, and XRD methods. Nanocellulose films had a density of up to 1.51 g/cm^3, a transparency of up to 82.4%, a carboxyl group content of up to 1.18 mmol/g, and a tensile strength of up to 69.7 MPa. The crystallinity index of nanocellulose decreases from 78.8 to 64.9% with an increase in the oxidation time. TEM and AFM methods have shown that the width of nanocellulose particles is from 3 to 20 nm. TGA confirmed a decrease in the crystallinity index of nanocellulose as a result of its prolonged oxidation. The properties of the obtained nanocellulose from ORP demonstrate the great potential of its application for the preparation of new nanocomposite materials.

Keywords Reed stalk · Organosolv pulp · Nanocellulose · TEMPO-mediated oxidation

Introduction

Recently, there has been a growing interest in the development of new biodegradable materials from environmentally friendly renewable plants. They are able to replace materials made from exhaustible natural resources—oil, gas, and coal. Polymers from these fossil fuels take hundreds of years to decompose, causing irreparable damage to the environment. Plastic accounts for 85% of all waste in the world's oceans, half of which are disposable plastic products (Jambeck et al. 2015; Schmidt et al. 2017). The use of natural polymers from plant materials is being seen as an alternative to plastics and could be a viable approach to reducing deforestation, increasing the use of agricultural surplus, and developing biodegradable materials.

The main component of plant raw materials is cellulose—the most widespread biopolymer on the Earth, which is widely used in the production of paper and cardboard, cellulose ethers and esters, microcrystalline cellulose, and oxycellulose (Dassanayake et al. 2018; Shaghaleh et al. 2018). Cellulose has also attracted considerable interest as a source of raw materials for the production of nanocellulose (NC). Nanocellulose is a new class of nanomaterials, which has unique properties, such as high elastic modulus, high specific surface area, optical transparency, low thermal expansion, nanoscalability, and biocompatibility and being a renewable and biodegradable material, that enable its use in many fields. Nanocellulose is used in optoelectronic (Thomas et al. 2018) and medicine (Alavi 2019), in the production of chemical current of sources and sorbents (Jasmani et al. 2018; Nazl et al. 2019), for reinforcing and improving the mechanical strength and/or barrier properties of polymeric (Trache et al. 2020), and cement and paper

✉ V. A. Barbash
v.barbash@kpi.ua

[1] Department of Ecology and Technology of Plant Polymers, National Technical University of Ukraine "Igor Sikorsky Kyiv Polytechnic Institute", Kiev, Ukraine

composites (Abdul-Khalil et al. 2014; Baghban et al. 2020; Charani et al. 2019).

The preliminary step for nanocellulose extraction is the pretreatment of lignocellulosic biomass to remove the lignin, hemicelluloses, and extractives. In the world pulp and paper industry, the dominant technologies of pulp production are the sulfate and sulfite methods, which lead to the environmental pollution of harmful toxic sulfur compounds (sulfur dioxide, hydrogen sulfide, and mercaptans). Environmental requirements for the quality of wastewater and gas emissions discharged by industrial enterprises stimulate the development of new technologies for processing plant materials using organic solvents (Phanthong et al. 2018; Sharma et al. 2019). Organic solvents perform the functions of both a chemical reagent and an environment in which the process of delignification of plant materials occurs. As a chemical reagent, organic solvents interact with structural units of lignin, which leads to its destruction or blocking of reactive groups (primarily benzyl alcohol) to prevent lignin condensation reactions. Organic solvents can belong to one or several classes of organic compounds—monohydric and polyhydric alcohols, phenols and carboxylic acids, ethers and esters, ketones and amines, peroxides. Their effect on plant raw materials is distinguished by the chemistry and technological parameters of the pulping process. Among organic solvents, acetic acid due to relatively low cost can be regarded as a potential agent to achieve extensive delignification. The application of hydrogen peroxide during pulping promotes delignification of raw materials; increased brightness can also be achieved by delignification with peroxy compounds. At the same time, less-pronounced impact on cellulose is observed during pulping with such compounds (Kumar et al. 2013). A solution of acetic or formic acid and hydrogen peroxide forms peracetic or performic acid, which, as a strong oxidizing agent, is characterized by excellent delignification and bleaching properties (Jahan et al. 2014). This acid is an environmentally friendly alternative to delignification and bleaching, because it is a totally chlorine-free process resulting in less damage to the fiber (Paschoal et al. 2015). Peracetic acid selectively dissolves lignin and minimally damages the carbohydrate components of raw materials (Choi et al. 2019; Esmaeil et al. 2019). This cooking process is carried out at low temperature that helps to consume low energy (Deykun et al. 2018).

The extraction of nanocellulose can be achieved using the following methods: mechanical treatment, acid and enzymatic hydrolysis, oxidation of cellulose, or their combination. The essence of the mechanical methods is an application of different forces to reduce the size of the natural cellulose fibers to nanoscale. For this, various mechanical processing is used: homogenization, grinding, microfluidization, ultrasonic treatments, ball milling, and cryocrushing (Rol et al. 2019). The use of mechanical methods for obtaining nanocellulose is characterized by significant energy consumption. To reduce energy consumption and fiber damage during mechanical processes, various pretreatments of cellulose are used: enzymatic treatment, alkaline treatment, and chemical oxidation. As a result of the rupture of strong interfibrillar hydrogen bonding, the power required for the production of NC is significantly reduced, for example, from 20–30 to 0.5 kW/kg of sulfite pulp (Klemm et al. 2005).

Chemical methods are based on the cleavage of 1–4 glycosidic bonds of cellulose chains and isolation of cellulose nanocrystals with the removal of a part of the amorphous cellulose under the action of acids. For these purposes, the different acids are used: sulfuric, hydrochloric, phosphoric, maleic, hydrobromic, nitric, formic, and *p*-toluenesulfonic (Biana et al. 2018; Mahmud et al. 2019). Sulfuric acid is most widely used to produce NC. It reacts with the surface hydroxyl groups of cellulose to form negatively charged sulfonic groups and a stable NC gel. Otherwise, upon hydrolysis with hydrochloric acid, uncharged nanocellulose particles tend to flocculate in aqueous dispersions (Kargarzadeh et al. 2017). The major drawback of this process is the acid-containing waste water which has to be treated before releasing to the environment. Deep eutectic solvents and ionic liquids can be potentially useful chemicals for the NC extraction. Their advantages are associated with a simple and efficient process of cellulose hydrolysis in a homogeneous environment (De Santi et al. 2012; Seta et al. 2020).

Enzymatic methods are based on the biosynthesis from monosaccharides or decreasing the size of the cellulose fibers by the fermentation. The enzymatic methods are time-consuming and require reagents that are more expensive compared to acid hydrolysis process. However, preliminary treatment of cellulose by enzymes before the mechanical grinding can decrease the energy consumption required for preparation of NC (Amezcua-Allieri et al. 2017; Long et al. 2017). For these reasons, a pretreatment of the fibrous material is usually performed to decrease the size of the cellulose fibers and to ease the fibrillation and the process of nanocellulose preparation. The method of NC production by combining mechanical, chemical, or biological pretreatment with homogenization treatment can not only reduce energy consumption, but also obtain NC with controllable size (Yang et al. 2019; Zhanga et al. 2020).

Oxidizing agents such as 2,2,6,6-tetramethylpiperidine-1-oxyl (TEMPO) and phthalimide-*N*-oxyl (PINO) are also used to prepare NC (Coseri et al. 2009; Madivoli et al. 2020). They improve the environmental friendliness and shorten the duration of the nanocellulose production process compared to hydrolysis, but have a higher cost than the above acids (Isogai 2018). TEMPO is a water-soluble and stable nitroxyl radical, and commercially available for laboratory and industrial use. A number of articles have

appeared on the use of TEMPO for the production of nanocellulose, mainly from wood cellulose (Asad et al. 2018; Banerjee et al. 2020; Levanič et al. 2020). Extracted NC is characterized by high dispersion in water due to a larger number of carboxylate groups, smaller nanoparticles, and a higher transmittance as compared to NC obtained using the conventional hydrolysis method (Hirota et al. 2010). For the practical application of such a technology for producing nanocellulose from various plant raw materials, it is necessary to continue the process of accumulating fundamental, experimental, and analytical data to increase its reliability at the industrial level.

The main raw material for cellulose production in the pulp and paper industry is wood. In recent decades, there has been a decrease in timber reserves, which leads to a violation of the ecological balance on the planet. For countries with limited wood resources, it is important to expand the fiber base using non-wood plant raw materials. Common reed (*Phragmites australis*) also belongs to such raw materials. Common reed is a cheap and common plant that grows on the banks of rivers and lakes as a result of the efficient use of solar energy utilization by means photosynthesis process. It is one of the most widespread wild-growing species of flowering plants in Europe, Asia, North Africa, and North and South America, is a tall up to 4 m perennial cereal (Saltonstall 2002). Common reed has the ability to form monospecific stands occupying large areas (Asaeda et al. 2006). Only in Ukraine, common reed harvesting averages 3200 tons per year and tends to grow. Reed stems can be used for the production of pulp, paper, and cardboard, but there are no data on the production of nanocellulose by TEMPO-mediated oxidation. Taking into account the fact that the market size for nanocellulose was close to USD 146.7 million in 2019 and will grow at a compound annual growth rate of 21.4% from 2020 to 2026, many lignocellulosic materials, including common reed, can be considered as feedstock for its production.

The aim of the study was to prepare pulp from reed stalks using an environmentally friendly organosolv method followed by its TEMPO-mediated oxidation to obtain nanocellulose and to study its properties to assess its potential application.

Experimental details

Materials and chemicals

We used the biomass of common reed from the Cherkassy region of Ukraine after the harvest in 2019. Before research, the raw material was crushed to 2–5 mm and stored in a desiccator to maintain a constant moisture content and chemical composition. The chemical composition of reed stalks was determined according to TAPPI standards to determine cellulose by Kurshner–Hoffener method with using of alcoholic nitric acid (T 249), lignin (T 222), hot water solubility (T 207), 1% NaOH solubility (T 212), alcohol–benzene solubility (T 204), and ash (T 211). The analyses for the chemical characterization were done in triplicate and the mean and standard deviation were calculated. *S*odium hydroxide, glacial acetic acid, hydrogen peroxide, ethanol, 2,2,6,6-tetramethylpiperidine-1-oxyl (TEMPO), sodium bromide, and sodium hypochlorite were chemical grade.

Cooking process

The pulp was obtained from reed stalks in two stages. At the first stage, an alkali solution was used as a preliminary treatment of plant raw materials to remove the main part of hemicelluloses and minerals and partially remove lignin. Carrying out alkaline pretreatment before organosolv cooking allows, taking into account the peculiarities of the chemical composition of raw materials, to reduce the amount of substances subject to destruction in the spent cooking solution and to increase the efficiency of its recycling (Vurasko et al. 2018). For this, the reed stalks were extracted with a NaOH solution with a concentration of 50 g/l at a temperature of 97 ± 2 °C for 120 and 180 min, the ratio of liquid-to-solid is 10:1. At the second stage, to remove residual lignin and extractives, organosolv cooking was carried out using a solution of glacial acetic acid and 35% hydrogen peroxide in a volume ratio of 7:3 with a liquid-to-solid ratio of 10:1 at a temperature of 97 ± 2 °C for 120 or 180 min. These values of technological parameters were previously determined for the extraction of wheat straw (Barbash et al. 2017a), flax (Barbash et al. 2017b), kenaf (Barbash et al. 2018), and miscanthus (Barbash et al. 2019). The obtained organosolv reed pulp (ORP) had traces of non-cellulosic components and was stored wet in an airtight bag to produce nanocellulose. Removal of residual lignin from organosolv pulp is necessary, because it prevents the oxidation of hydroxyl groups at C6, reduces the crystallinity of nanocellulose, and negatively affects the thermal stability and transparency of nanocellulose films (Chen et al. 2018). Residual lignin will also interfere with the nanocellulose production process when the pulp is exposed to acid solutions, which will lead to condensation of lignin. Never dried pulp is better for obtaining nanocellulose, as dried samples irreversibly lose access to the surface during the drying process. Using never-dried pulp does not require consumption of energy for drying and grinding, since dried cellulose fibers lose the ability to swell and percolate due to irreversible cornification (Barbash et al. 2020).

Preparation of TEMPO-oxidized nanocellulose

The nanocellulose has been prepared by TEMPO-mediated oxidation using the TEMPO/NaBr/NaOCl system followed by ultrasonic treatment. This treatment leads to the selective removal of the amorphous regions of cellulose while maintaining the crystalline regions of cellulose macromolecules (Sun et al. 2015; Yang et al. 2019). To obtain nanocellulose, 1 g of ORP was transferred into a beaker, 100 ml of distilled water was added, and the resulting aqueous suspension of cellulose was mixed with 0.16 g of sodium bromide and the required amount of TEMPO at the rate of 0.8–2.0% by weight of ORP. To uniformly impregnate cellulose suspension with these reagents, we used sonication in the ultrasound disintegrator UZDN-A (SELMI) at 22 kHz for 5 min. A solution containing NaClO at 10 mmol/g ORP is added to the slurry at room temperature and pH 10 to start the TEMPO-mediated oxidation, with continuous addition of 0.5 M NaOH to maintain the mixture at pH 10. The NaClO consumption of 10 mmol/g was used based on our preliminary studies and the results obtained by Lu et al. (2018) and Patiño-Maso et al. (2019), which show that the carboxyl content in the prepared TEMPO-oxidized nanocellulose increased with increasing NaClO consumption from 4 to 25 mmol/g. The duration of the TEMPO oxidation was from 2 to 24 h. To stop the TEMPO-oxidation process, we added 100 ml ethanol. Then, the suspension was centrifuged from TEMPO, salts, and other compounds present in the oxidizing mixture three times with the addition of distilled water at 4000 rpm for 10 min each. Ultrasonic treatment of a suspension of nanocellulose oxidized by TEMPO was carried out for 10–30 min until a transparent nanocellulose gel was formed. The resulting nanocellulose suspension was poured into Petri dishes and dried in air at room temperature to obtain NC films.

Methods of analyses

Scanning electron microscopy (SEM) studies were carried out on PEM–106I (SELMI, Ukraine) microscope to observe the morphology of reed pulps and nanocellulose films. The samples were sputter-coated with a layer of gold using the sputtering technique. Fourier-transform infrared spectroscopy (FTIR) spectra of the reed stalks, pulps, and nanocellulose films were recorded on Tensor 37 Fourier-transform infrared spectrometer with a 2 cm^{-1} resolution in the 400–4000 cm^{-1} frequency range. X-ray diffraction analysis (XRD) was carried out using an Ultima IV diffractometer (Rigaku, Japan) to determine the relative amount of the crystalline phase in samples of plant material, reed pulps, and nanocellulose films. Crystallinity index (CI) was calculated using Segal method (Segal et al. 1959):

$$\mathrm{CI},\ \% = \left[\left(I_{200} - I_{\mathrm{am}}\right)/I_{200}\right] \cdot 100, \tag{1}$$

where I_{200} is an intensity of (200) reflex for the crystalline phase at 2θ between 22° and 24°, and I_{am} is an intensity in the valley between the peaks of the amorphous region at 2θ between 18° and 19°.

Average crystallite size D or, more accurate, size of coherent-scattering regions in the direction of the normal to the reflecting planes, of the NC films was determined from the X-ray line broadening method using the Scherer's formula (Torlopov et al. 2017):

$$D = (k \cdot \lambda)/(\beta \cdot \cos\theta), \tag{2}$$

where k is the Scherer constant ($k = 0.94$); $\beta = (B–b)$ or $\beta = (B^2–b^2)^{0.5}$, when B is the observed full width at half maximum (FWHM), and b is the broadening in the peak due to the instrument in radians, and θ denotes the Bragg's angle of the X-ray diffraction peaks (110) and (200).

Transmission electron microscopy (TEM) was used to study the morphology of nanocellulose suspension. For these observations, TEM SELMI EMV-125 was used, for which an NC sample was prepared by dispersing 2 µl of an appropriate nanocellulose suspension in distilled water with a volume of 1–18 µl. Then, this dispersion was dropped onto copper grid coated by 5–10 nm-thick carbon film and dried in air for 15 min. TEM and electron diffraction analyses were fulfilled at room temperature using accelerating voltage of 75 kV. The diameters and lengths of the NC cellulose nanoparticles were determined using an image analysis program ImageJ 1.37v®, a minimum of 500 measurements performed for each determination.

Atomic force microscopy (AFM) was used to determine the topographic characteristics of nanocellulose samples.

Measurements were accomplished with Si cantilever, operating in a tapping mode on the device Solver Pro M (NT-MDT, Russia). The scanning speed and area were 0.6 line/s and 2×2 μm^2, respectively.

The transparency of the nanocellulose films was determined by the electron absorption spectra, which were registered in the range of 200–1100 nm. The electron absorption spectra of the nanocellulose films in UV and in visible and near-infrared regions were registered on two-beam spectrophotometer 4802 (UNICO, USA) with a resolution of 1 nm.

The content of carboxyl groups in nanocellulose was determined by the calcium acetate method according to the method described by Milanovich et al. 2012. A cellulose sample (0.5 g) was treated with 0.01 M HCl for 1 h, followed by washing with distilled water. Then, 50 ml of distilled water and 30 ml of 0.25 M calcium acetate solution were added to the fiber suspension. After standing for 2 h with frequent shaking, 30 ml portions of the

suspension were titrated with 0.01 M sodium hydroxide using a phenolphthalein indicator. The carboxyl contents are calculated as:

$$\text{COOH, mmol/g} = 80/30 \cdot 0.01\ M \cdot V_{\text{NaOH}}/m \cdot k, \quad (3)$$

where 0.01 M is concentration of NaOH, V_{NaOH} is volume (ml) of NaOH solution used for titration, m is weight of treated fibers (g), and k is content of absolutely dry matter in cellulose.

Thermogravimetric analysis (TGA) using a Netzsch STA-409 thermal analyzer was used to study the thermal destruction of reed pulps and nanocellulose samples. The samples were heated at a rate of 5 °C/min, from 25 to 450 °C. The weight of samples was within 0.25 ± 0.01 g, reference substance—α-corundum, crucible material—alund. Deviations of weight were registered and processed according to a program involving the use of computer technology. Based on the changes in the gravimetric and differential curves of thermal analysis, the initial temperature of the mass weight loss of reed pulps and NC samples were determined.

The density of nanocellulose films was determined according to ISO 534:1988. The tensile strength of the NC films was measured at a controlled temperature (23 ± 1 °C) and humidity (50 ± 2%) according to ISO 527-1. Tension tests were performed at a crosshead speed of 0.5 mm/min on the TIRAtest-2151 (Germany) instrument equipment with a 2-*N* load stress. For testing, test strips with 10 ± 2 mm width and 25 ± 5 mm long were used. The tensile strength of the NC films was calculated on five test pieces, expressing the results as an average and standard deviation.

The yield of the NC was determined as described by Besbes et al. (2011). A 0.1 wt % NC suspension was centrifugated at 10,000 rpm for 10 min to achieve the separation of the nanofibrillar material and non-nanofibrillated material. The sediments (non-nanofibrillated fraction) were dried to a constant weight at 100 °C. The yield is calculated from the next equation:

$$\text{Yield, \%} = \left[1-\left(W_S/\left(W_{NC} \cdot C_{NC}\right)\right)\right] \cdot 100, \quad (4)$$

where W_S weight of sediments; W_{NC} weight of NC suspension; C_{NC} concentration of NC suspension.

Results and discussion

Alkali treatment and pulping

Chemical analysis of plant materials showed that reed stalks had the following content of components: 49.3 ± 1.2% of cellulose, 22.9 ± 0.7% of lignin; hot water solubility—10.6 ± 0.3%; 1% NaOH solubility—19.4 ± 0.6%; 2.3 ± 0.3% of resin, fats, and waxes; 3.5 ± 0.5% of mineral substances (ash) relative to mass of dry raw material. Thus, the studied non-woody plant material contains less lignin than wood of coniferous and deciduous species, which a priori suggests a lower consumption of reagents and a shorter duration of the process of its delignification in comparison with obtaining pulp from wood. The change in the content of the main components of plant materials after the first and second stages with different thermochemical processing times is shown in Table 1.

The data in Table 1 show a regular decrease in all indicators of reed pulps with an increase in the duration of treatment both at the first and at the second stages. After 120 and 180 min of alkaline treatment, the content of lignin in the reed pulp decreased by only 36.7% and 46.7%, respectively, and the content of mineral substances by 79.6% and 75.1%, respectively, compared to the initial plant raw material. However, to obtain cellulose suitable for chemical processing, in particular for the production of nanocellulose, additional chemical treatment is required. As can be seen from the data (Table 1), this is achieved by organosolv cooking. Thus, carrying out alkaline treatment and cooking for 180 min allows to obtain the ORP with a lower content of residual lignin and traces of minerals, which was used to obtain nanocellulose. Such values of the ORP quality indicators are close to the indicators of organosolv pulps obtained as a result of these two stages of thermochemical treatment of other representatives of non-wood plant raw materials, such as wheat straw, flax, kenaf, and miscanthus (Barbash et al. 2017a, b, 2018, 2019, 2020).

Morphology of reed pulp

The morphology of the initial plant raw material and the reed pulps after stages I and II was studied using SEM (Fig. 1). As seen from Fig. 1a, the initial reed stalk consists of several layers of fibrils with a dense structure and a smooth surface. In the course of alkaline treatment, the reed stalks are partially separated into fibers with a residual content of lignin and extractives (Fig. 1b). Changes in the structure of reed fibers in the process of organosolv cooking are shown

Table 1 The indicators of the reed pulp after stages of its processing (%)

Pulp indicators	Pulp after alkali pretreatment for		Pulp after the peracetic cooking for	
	120 min	180 min	120 min	180 min
Yield	66.5 ± 1.7	58.0 ± 1.5	70.7 ± 2.1	63.8 ± 1.9
			46.6[a] ± 1.4	37.0[a] ± 1.2
Lignin	14.5 ± 0.9	12.2 ± 0.7	0.53 ± 0.05	0.39 ± 0.04
Ash	1.03 ± 0.07	0.87 ± 0.04	0.03 ± 0.004	0.02 ± 0.003

[a]Regarding to original raw material

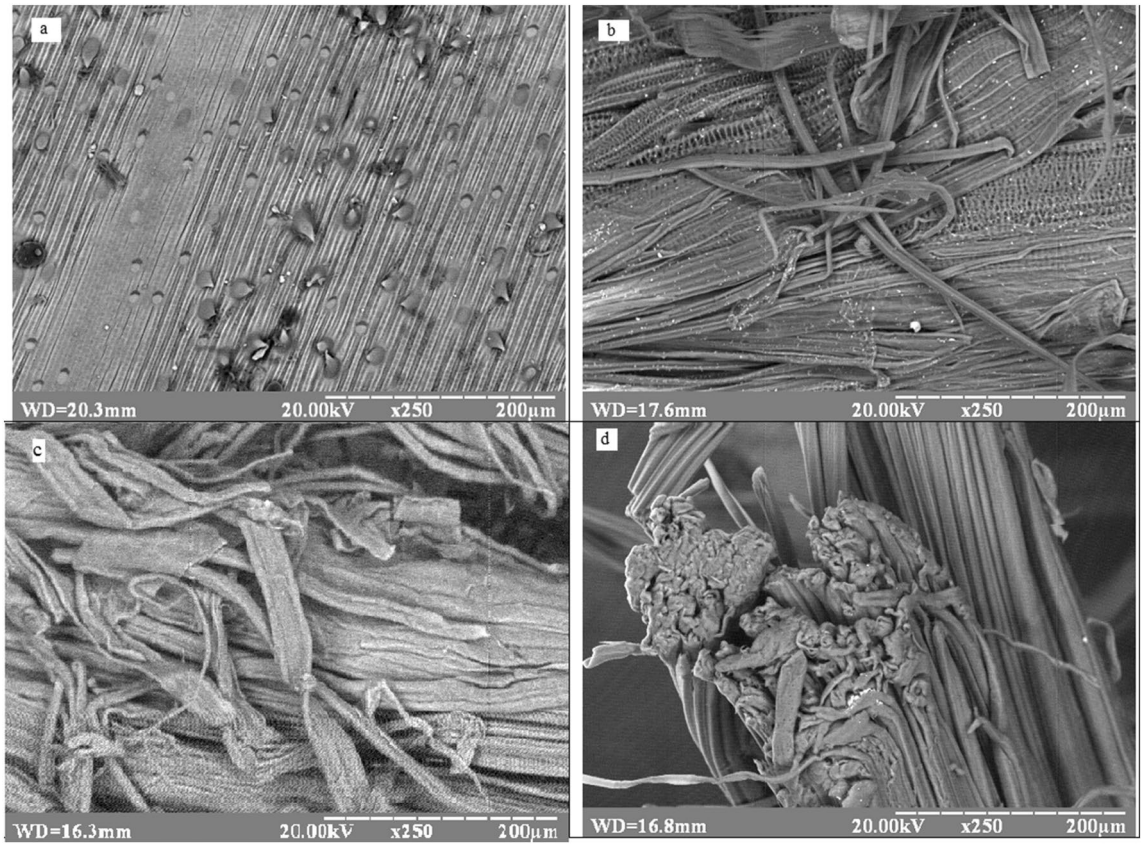

Fig. 1 SEM images. **a** Reed stalk; **b** pulp after alkali treatment; **c** pulp after cooking; **d** cross section of ORP

in Fig. 1c. Acidification of fibers in a mixture of acetic acid and hydrogen peroxide promotes the separation of stalks into fibrils due to the destruction of internal bonds between lignin and hemicellulose molecules, while hydrogen peroxide helps to bleach the reed pulp (Fig. 1c). Cross-sectional electron micrographs of ORP show its separation into smaller fibrils as a result of the removal of the remaining non-cellulosic components (Fig. 1d). The length of the original fibers of the reed varies and reaches several millimeters, but after thermochemical treatment, the length of the fibers of the ORP decreases to 100–800 microns. Reed fibers are more than 20 µm wide, and after alkaline treatment and peracetic cooking, they decrease to 20 and 10 µm, respectively (Fig. 1d).

Chemical composition of ORP and NC

The change of chemical composition of ORP in the process of its thermochemical treatment was confirmed by infrared spectroscopy. Figure 2 shows the Fourier IR spectra of the reed stalks, pulps after alkaline treatment and cooking, and nanocellulose after TEMPO-mediated oxidation. All spectra are characterized by a wide band width in the region of 3000–3800 cm^{-1}, which corresponds to stretching vibrations of hydroxyl groups included in intramolecular and

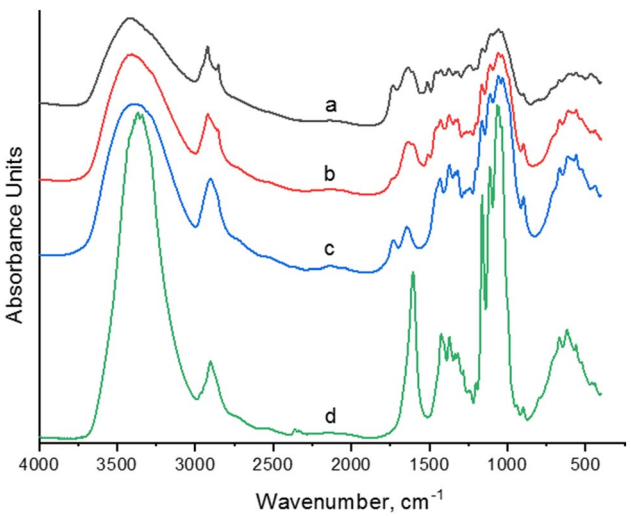

Fig. 2 FTIR spectra of different samples **a** of reed stalk; **b** pulp after alkaline treatment and **c** pulp after cooking; **d** nanocellulose film

intermolecular hydrogen bonds. The bands in the area of 3000–2800 cm^{-1} correspond to the asymmetric and symmetric stretching vibrations of the $–CH_2$, –CH, and hydroxyl groups. Their number naturally decreases in the course of

thermochemical processing of raw material, as evidenced by a decrease in intensity peaks in this area. In the Fourier IR spectra of reed pulps after stages I and II (Fig. 2b, c), in comparison with the spectrum of the initial plant raw material, there is a decrease in the intensity of bands in the region of 1500–1800 cm^{-1}, which characterize the bands of stretching vibrations of double bonds. Vibration bands in the 1740 cm^{-1} region indicate the presence of a carbonyl group characteristics of hemicelluloses. As can be seen from Fig. 2b, alkaline treatment significantly removes hemicelluloses from the cellulose composition, but subsequent organosolv cooking increases the amount of carbonyl groups due to oxidation by hydrogen peroxide. A decrease in the intensity of vibrations in the region of 1600 cm^{-1}, which is characteristics of aromatic compounds—residual lignin, indicates a removal of lignin from plant material and pulp during their thermochemical treatments (Fig. 2a–c). An increase in the intensity of the band from the maxima of 1600 cm^{-1} for nanocellulose (Fig. 2d) indicates a significant increase in the number of carboxyl and carbonyl groups due to the oxidation of hydroxyl groups in C6 under the action of the TEMPO-mediated oxidation. In the region 1200–1450 cm^{-1}, absorption bands are located due to bending vibrations of the angles and bonds of the CH_2OH group at C6 of cellulose. The band in the region of 1430 cm^{-1} is due to the deformation vibrations of the CH_2 groups, and the bands at 1360 and 1340 cm^{-1} are due to deformation vibrations of hydroxyl groups. The band at 1160 cm^{-1} is due to the asymmetric vibrations of the C–O bonds, while the band at 1060 cm^{-1} corresponds to the vibrations of the C–O–C bridge of the glucopyranose ring of cellulose (Ilyas et al. 2017). The increase of the intensity of the bands in the region of 1050, 1400, and 3400 cm^{-1} demonstrates the efficiency of removal of lignin and noncellulose components from the plant feedstock in the investigated sequence of thermochemical treatments.

TEMPO-oxidation process

TEMPO-oxidized nanocellulose (TONC) suspension was extracted from ORP using TEMPO/NaBr/NaClO oxidation system followed ultrasonic treatment. The effect of the TEMPO oxidizer consumption on the quality indicators of the obtained nanocellulose films during the oxidation process for 4 and 20 h is shown in Fig. 3. As shown in Fig. 3 data, an increase in the consumption of the oxidizing agent and the duration of the oxidation process contributes to an increase in the density and tensile strength of nanocellulose films. The change in the density of TONC films is associated by a decrease in the size of cellulose fibers in the process of TEMPO-mediated oxidation with their transformation into nanoparticles, which form denser structures with stronger bonds between them. The dependence of the TONC properties on the oxidation time at the TEMPO consumption of 1.6% of the ORP mass is presented in Table 2. The data in Table 2 show that an increase in the duration of the oxidation process contributes to the production of TONC films with a higher density and a high content of carboxyl groups, as well as an increase in their transparency and mechanical strength. It was found that an increase in the oxidation time reduces the yield of nanocellulose due to the destruction of cellulose macromolecules by prolonged action of the oxidizing agent.

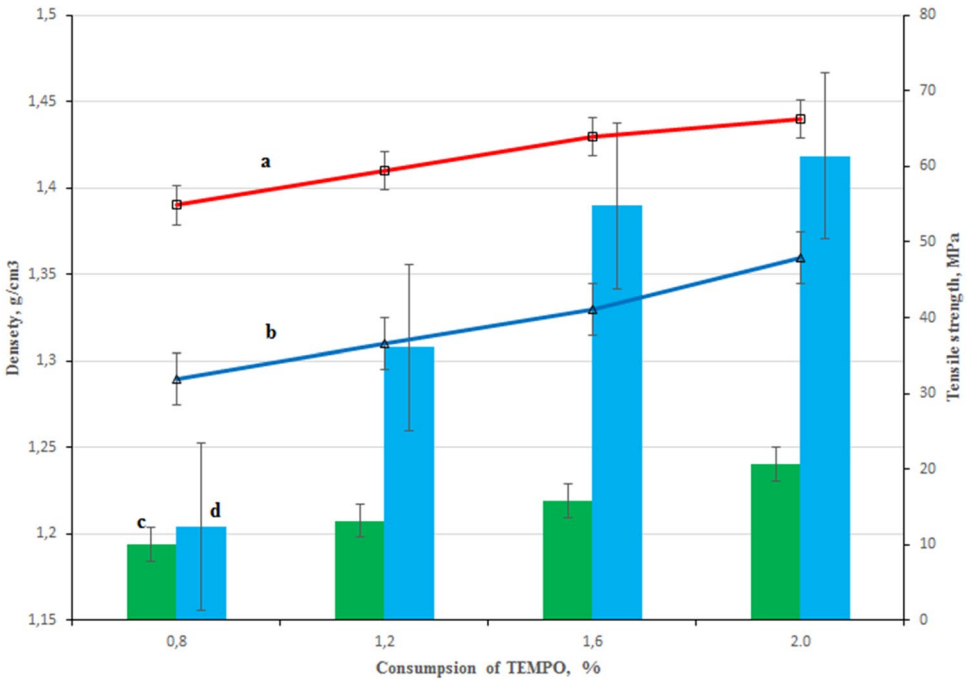

Fig. 3 Dependence of nanocellulose properties on TEMPO consumption during 4 h (b, c) and 20 (a, d) hours of oxidation. Density (a, b); tensile strength (c, d)

Table 2 Dependences of nanocellulose properties on oxidation time

Time of oxidation, hours	Yield, (%)	Density, (g/cm^3)	Tensile strength, MPa	Content of COOH, (mmol/g)	Transparency, (%)
0	100	0.53 ± 0.01	1.73 ± 0.1	0.12 ± 0.02	–
2	75.4 ± 2.7	0.75 ± 0.02	5.05 ± 0.2	0.23 ± 0.03	28.5 ± 0.8
4	58.7 ± 2.2	0.90 ± 0.02	12.5 ± 0.5	0.39 ± 0.07	35.7 ± 1.2
8	42.8 ± 2.1	1.12 ± 0.03	21.5 ± 0.8	0.43 ± 0.10	52.2 ± 2.6
15	41.2 ± 2.0	1.28 ± 0.03	42.8 ± 1.1	0.74 ± 0.15	68.4 ± 3.3
18	40.4 ± 1.9	1.37 ± 0.04	53.2 ± 1.8	0.90 ± 0.18	72.8 ± 3.7
20	38.7 ± 1.8	1.48 ± 0.04	58.5 ± 2.5	1.01 ± 0.22	78.3 ± 3.9
24	36.5 ± 1.8	1.51 ± 0.05	69.7 ± 3.2	1.18 ± 0.23	82.4 ± 4.2

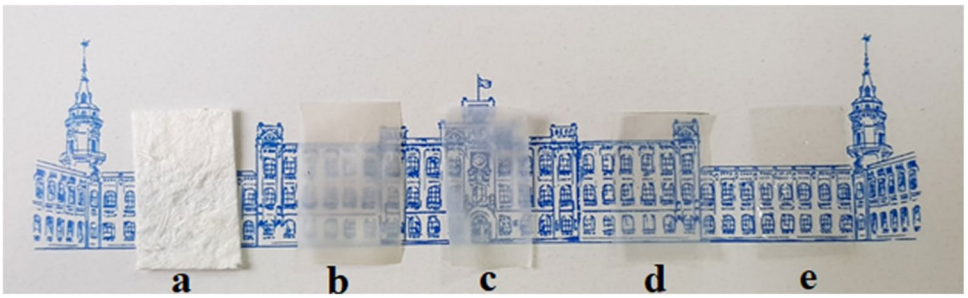

Fig. 4 Comparison of transparent strips made from: **a** initial ORP, **b** TONC film after the oxidation 2 h, **c** TONC film after the oxidation 4 h, **d** TONC film after the oxidation 8 h, and **e** TONC film after the oxidation 24 h

In this case, there is a sharp decrease in the yield of nanocellulose in the first 4 h of ORP oxidation (up to 58.5%) and a slight decrease in its yield with a subsequent increase in the oxidation time.

This occurs due to the dissolution and removal during the washing process of low molecular weight, primarily amorphous parts of nanocellulose. This leads to a decrease in the size of cellulose fibers in the process of TEMPO-mediated oxidation with their transformation into nanoparticles, which form denser structures with stronger bonds between them. In this case, the density of TONC increases by three times, and the tensile strength by 40 times compared with these indicators for ORP. Changes in the look of ORP and TONC films according to the duration of TEMPO-mediated oxidation are presented in Fig. 4.

Comparison of the strips shows that the films obtained with long exposure in the TEMPO/NaBr/NaClO system on an ORP have higher transparency. These results show that prolonged treatment of ORP with TEMPO-mediated oxidation leads to the formation of homogeneous TONC films with high density up to 1.51 g/cm^3 and high transparency up to 82.4% at a wavelength of 600 nm (Table 2).

The prepared TONC looked like a homogeneous and stable suspension (Fig. 5). The nature of stabilization of the colloidal suspension is explained by the presence of charged groups on the surface of nanocellulose, which are formed by the interaction of cellulose with TEMPO/NaBr/NaClO system due to the esterification reaction.

Fig. 5 Photographs of vials with nanocellulose suspensions prepared after 24 h of TEMPO-mediated oxidation of ORP: **a** without ultrasonic treatment; **b** after ultrasonic treatment, and **c** after 4 months of storage

Confirmation of the stability of the nanocellulose suspension is the absence of sedimentation of nanocellulose particles after preparation and after long-term storage at room temperature. The obtained transparency values are in good agreement with the known data (Zhu et al. 2013; Patiño-Maso et al. 2019), which show an increase in the transmission of the nanocellulose suspension with an increased TEMPO consumption.

As can be seen from the data in Table 2, with an increase in the oxidation time from 2 to 24 h, the content of carboxyl groups increases from 0.12 mmol/g in ORP to 1.18 mmol/g in TONC. That is, the content of carboxy groups increases by about 10 times as compared to the initial ORP. This indicates that the oxidation process occurs in the C6–OH groups both on the surface of crystalline cellulose microfibrils and in the C6–OH groups inside cellulose microfibrils. The obtained values of the content of carboxyl groups are in the range of known values. For example, after TEMPO oxidation of bleached bagasse pulp with a consumption of NaClO 4, 6 and 8 mmol/g, nanocellulose was obtained with a content of carboxyl groups of 0.73, 1.08, and 1.29 mmol/g, respectively (Lu et al. 2018). Patiño-Maso et al. (2019) prepared TEMPO-oxidized nanocellulose from in baby diapers with a consumption of NaClO 5, 10, 15, and 25 mmol/g, and obtained carboxy content values were 0.78, 1.17, 1.31, and 1.35 mmol/g, respectively. TEMPO oxidation of bleached softwood kraft pulp with NaClO consumption up to 20 mmol/g increases the content of carboxyl groups in nanocellulose to 1.7 mmol/g (Isogai 2018). An increase in the content of carboxyl groups is associated with an increase in the access of reagents to internal microfibrils of cellulose during TEMPO oxidation and is confirmed by changes in the crystal structure of cellulose I obtained by X-ray diffraction analysis.

Crystallinity of ORP and TONC

The X-ray diffractograms of initial reed stalks, pulp after treatment with alkali at 95 °C and at 160 °C, and ORP and TONC after different time of TEMPO oxidation are depicted in Fig. 6. Based on the analysis of diffraction patterns and changes in the ratio of the amorphous and crystalline parts of the samples under study, their crystallinity index (CI) was calculated.

X-ray diffraction patterns show that all studied samples consist of both crystalline and amorphous domains, which tend to influence the observed pattern and values of the crystallinity index (CI). The diffraction pattern of cellulose isolated from reed stems (Fig. 6A, a) consisted of crystalline cellulose domains with peaks at 2θ angles of 16º, 22º, and 34º, which were assigned to the diffraction planes (101), (200), and (040), respectively (Saberikhan et al. 2011). As can be seen from the data in Fig. 6A, the values of the cellulose crystallinity index gradually decrease as the thermochemical treatment proceeds. This pattern of decreasing CI is associated with an increase in the destruction of the carbohydrate complex of plant raw materials with an increase in the influence of temperature and chemicals. An illustration of this is the lower value of the crystallinity index of pulp after alkaline treatment under the influence of a higher temperature on the raw material: CI = 73.4 at 160 °C compared to CI = 75.9 at 95 °C (Fig. 6A, c and b). The subsequent decrease in the value of the CI of pulp after cooking is associated with the oxidative effect of hydrogen peroxide, which is part of the cooking solution, on cellulose fibers (Fig. 6A, d). It has been established that the crystallinity index of reed pulp decreases in the following order: initial raw material—pulp after alkaline treatment at 95 °C—pulp after alkaline treatment at 160 °C—ORP. The obtained crystallinity index of the ORP is 72.8%, which is higher than for organosolv straw pulp (CI = 64.1%) produced by Sánchez et al. 2016 and is the same (CI = 72.5%) as that obtained for organosolv straw pulp (Barbash et al. 2017a).

After a short duration of the TEMPO oxidation of the ORP (2 h), the CI of the nanocellulose increases from 72.8 to 78.4% due to the destruction of the amorphous part of the cellulose. However, with a subsequent increase in the

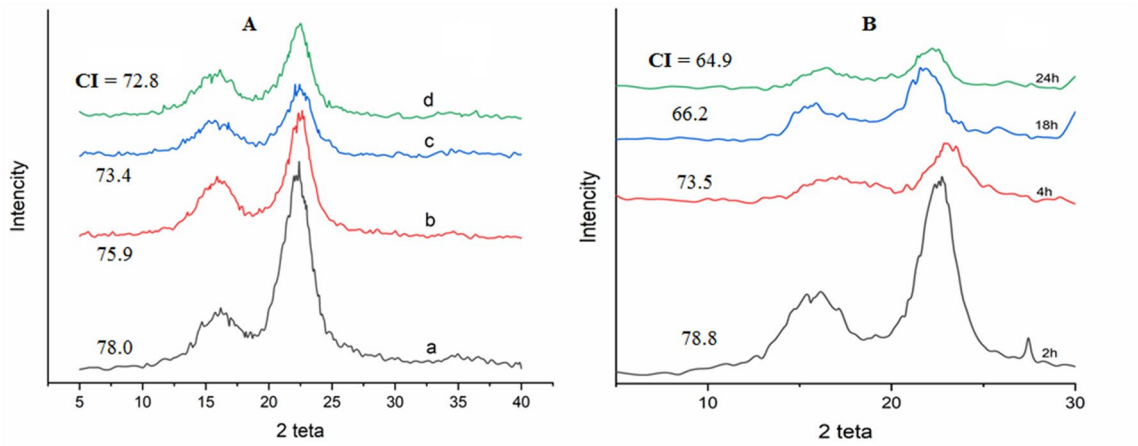

Fig. 6 X-ray diffractograms. **a**—a reed stalks; b reed pulp after treatment with alkali at 95 °C; c reed pulp after treatment with alkali at 160 °C; d ORP; **b** TONC after different time of oxidation

duration of TEMPO-mediated oxidation, a decrease in the amplitude of the intensity peaks of the crystalline part of cellulose is observed in the TONC diffractograms. Thus, with an increase in the oxidation time, there is a tendency to a decrease in the crystallinity index of TONC (Fig. 6b). A decrease in the value of the crystallinity index of TONC is also associated with the action of ultrasonic treatment on it due to the partial destruction of the crystalline regions of cellulose macromolecules under the influence of high ultrasound energy. Shak et al. noted decomposition of nanocellulose under the influence of TEMPO-mediated oxidation (Shak et al. 2018).

Values of the average crystallite size D of TONC estimated using Eq. (2) from (110) and (200) reflexes of XRD pattern in Fig. 6b are 2 and 3 nm, respectively. They all are similar to D values obtained for different nanocellulose samples by Plermjai et al. 2010 and Torlopov et al. 2017. To refine and analyze the particle size after oxidation, we studied the morphology of TONC samples using TEM and AFM.

Dimensions of TONC

The TEM analysis data of the TONC suspension show its multilayer structure with a fine network of nanocellulose particles as a result of interaction between them (Fig. 7). The morphology of the nanocellulose suspension differed in its dense and subtle regions, depending on the degree of dilution of the initial suspension with water. This phenomenon is explained by the inhomogeneous distribution of the amorphous and crystalline phases of nanocellulose in an aqueous medium (Sosiati et al. 2017). As seen in Fig. 7a, when using a concentrated suspension, TEM image of the dense region of TONC demonstrates nanoparticles with elongated rod-like shape, specifically, nanoparticles with average width from 4 to 10 nm. Such shape of cellulose nanoparticles is typical for that obtained from plant biomass by TEMPO oxidation (Madivoli et al. 2020) and by the hydrolysis of cellulose using sulfuric acid (Shak et al. 2018; Feng et al. 2017). Isogai showed that TEMPO-mediated oxidation converts wood cellulose fibers into nanofibers about 3 nm wide (Isogai 2018). As it is supported by the electron diffraction pattern in the inset in Fig. 7a, these nanoparticles are mainly composed of cellulose nanocrystals.

When the nanocellulose suspension was diluted with water, no agglomeration of nanoparticles occurred, which is explained by the presence of residues of anionically charged carboxylate groups in nanocellulose obtained by TEMPO-mediated oxidation (Sun et al. 2015). Instead, the diluted suspension TONC created networks with average width in the 5–40 nm range and length up to 0.8 µm (Fig. 7b). Similar networks of fine cellulose nanofibrils through TEMPO-mediated oxidation of cellulose obtained Abitbol et al. 2016 and Gopakumar et al. 2019.

These dimensions of TONC correspond to data obtained by AFM (Fig. 8). As shown in Fig. 8a, nanocellulose particles aggregated and interlaced. The transverse size of nanocellulose particles is in the range of 5–20 nm, but individual nanofibers are up to 28 nm wide and up to several micrometers in length (Fig. 8a). Such values of the sizes of TONC are confirmed by the data obtained for other representatives of non-woody plant raw materials. For example, the width of nanocellulose obtained by hydrolysis of organosolv pulp from wheat straw was 10–45 nm (Barbash et al. 2017a, b), from kenaf—10–28 nm (Barbash et al. 2019), from flax—15–65 nm (Barbash et al. 2018), from miscanthus—10–20 nm (Barbash et al. 2019), and from bleached sulfate softwood pulp—15–30 nm (Barbash et al. 2016).

Thermal stability

The effect of temperature on the stability of cellulose samples was investigated by thermogravimetric analysis (TGA). It was established that the temperature dependences of the weight loss of reed pulp after the alkali treatment and cooking have a similar character (Fig. 9). Thus, when these samples are heated from room temperature to a temperature of 250 °C, a gradual loss of their weight up to 15% is observed due to the evaporation of water and partial pulp

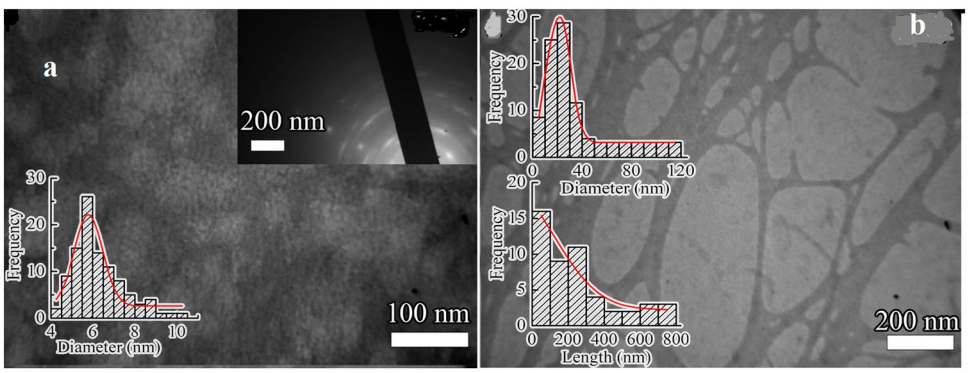

Fig. 7 TEM images of TONC suspension **a** in dense region; **b** in subtle region. Inset **a** shows an electron diffraction pattern of TONC. Left insets in **a** and **b** show the nanoparticle size distributions in the corresponding TONC suspensions

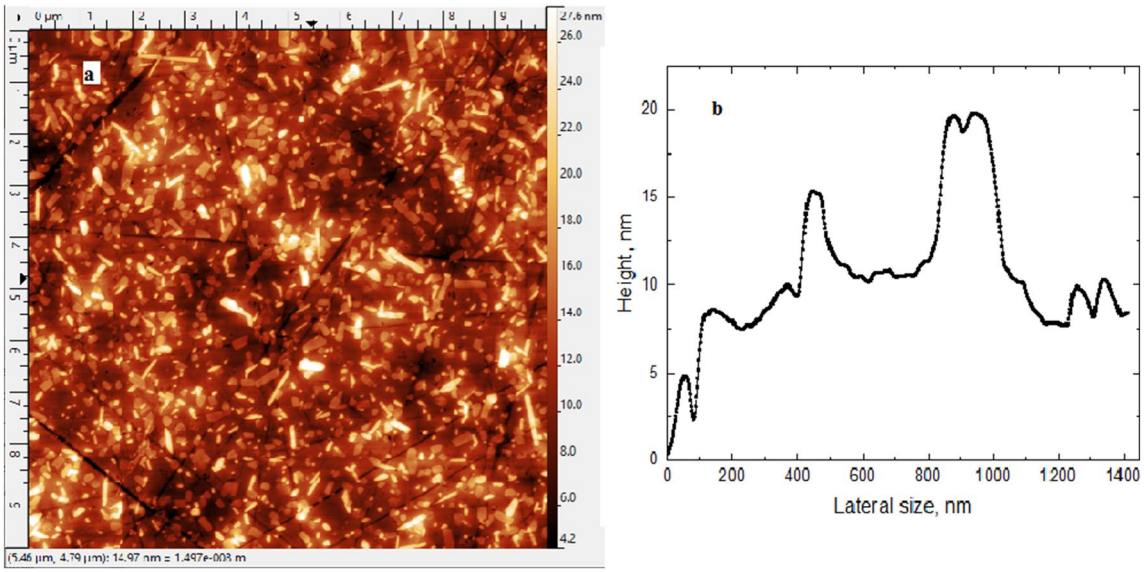

Fig. 8 **a** AFM image of a nanocellulose film in height; **b** amplitude in the tapping mode

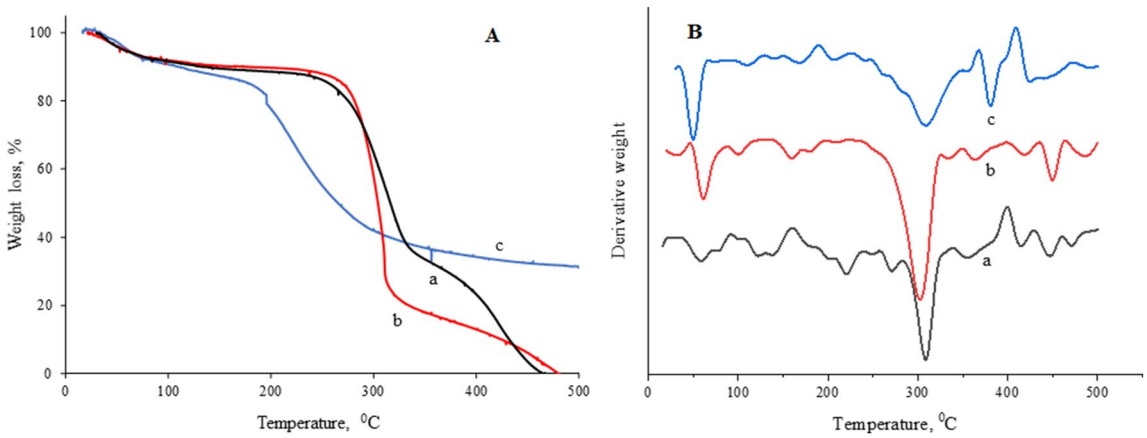

Fig. 9 **a** Gravimetric and **b** differential curves of thermal analysis. a Reed pulp after the alkali treatment; b ORP; c nanocellulose films

destruction (Fig. 9A, a, b). A further increase in temperature to 300–350 °C leads to a sharp decomposition of pulp and a weight loss of up to 60% for pulp after NaOH treatment and up to 80% for ORP. At 450 °C, these samples lose about 90% of their initial weight.

Another character of the weight change due to heating is observed for the TONC samples. When heated to a temperature of 200 °C, a gradual weight loss of up to 20% is observed the initial weight, which indicates both the removal of adsorbed moisture and the partial destruction of nanocellulose. An increase in temperature to 300 °C leads to a sharp weight loss of the nanocellulose sample up to 60% of the initial one. A further increase in temperature to 500 °C reduces weight by only 10%. This character of the dependence of the weight loss of a nanocellulose sample on temperature indicates that it contains up to 20% of adsorbed moisture and about 40% of amorphous (less thermally stable) and 40% crystalline (more thermally stable) regions of nanocellulose. Thus, TGA confirmed a decrease in the crystallinity of nanocellulose as the result of prolonged treatment of ORP by TEMPO-mediated oxidation.

It should be noted that the presence of an amorphous part in the resulting nanocellulose makes it more flexible and expands the scope of its application (Dias et al. 2020). The properties of the obtained nanocellulose from ORP demonstrate the great potential of its application for the production of new nanocomposite materials, for example, in optoelectronic devices, packaging, and construction.

Conclusion

The organosolv pulp from reed stalks was prepared by the environmentally safer alkali treatment and organosolv cooking in a solution of peracetic acid. The obtained organosolv reed pulp (ORP) had traces of non-cellulosic substances and was used for the preparation of nanocellulose. It has been established that the crystallinity index of reed pulp decreases in the following order: initial raw material—pulp after alkaline treatment at 95 °C—pulp after alkaline treatment at 160 °C—ORP. ORP is completely converted to nanocellulose particles by 2,2,6,6-tetramethylpiperidine-1-oxyl (TEMPO)-mediated oxidation in the TEMPO/NaBr/NaClO system followed by ultrasonic treatment to obtain a stable nanocellulose gel. It was found that an increase in the TEMPO consumption and oxidation time increases the density and tensile strength, the content of carboxyl groups, and the transparency of the nanocellulose films, but decreases the yield and crystallinity of the nanocellulose. Structural and chemical changes and the crystallinity index of reed stalks, ORP, and nanocellulose were studied using SEM, FTIR, and XRD methods. Nanocellulose films had a density of up to 1.51 g/cm^3, a transparency of up to 82.4%, a carboxyl group content of up to 1.18 mmol/g, and a tensile strength of up to 69.7 MPa. The crystallinity index of nanocellulose decreases from 78.8 to 64.9% with an increase in the oxidation time. TEM and AFM methods have shown that the width of nanocellulose particles is from 3 to 20 nm. TGA confirmed a decrease in the crystallinity of nanocellulose as the result of prolonged TEMPO oxidation. The properties of the obtained nanocellulose from ORP demonstrate the great potential of its application for the preparation of new nanocomposite materials, for example, in optoelectronic devices, packaging, and construction.

Acknowledgements The authors are grateful to the Ministry of Education and Science of Ukraine for funding the work and express their sincere gratitude to Dr. Natalia Klochko and colleagues from NTU "Kharkiv Polytechnic Institute" and V. N. Karazin Kharkiv National University for assistance in TEM and XRD investigations.

Compliance with ethical standards

Conflict of interest The authors declare that they have no competing interests.

References

Abdul-Khalil HP, Davoudpour Y, Nazuruyl Islam M, Asniza M, Sudesh K et al (2014) Production and modification of nanofibrillated cellulose using various mechanical processes: a review. Carbohydr Polym 99:649–665

Abitbol T, Rivkin A, Cao Y, Nevo Y, Abraham E, Ben-Shalom T, Lapidot S, Shoseyov O (2016) Nanocellulose, a tiny fiber with huge applications. Curr Opin Biotechnol 39:76–88. https://doi.org/10.1016/j.copbio.2016.01.002

Alavi M (2019) Modifications of microcrystalline cellulose (MCC), nanofibrillated cellulose (NFC), and nanocrystalline cellulose (NCC) for antimicrobial and wound healing applications. E-Polymers 19:103–119

Amezcua-Allieri MA, Durán TS, Aburto J (2017) Study of chemical and enzymatic hydrolysis of cellulosic material to obtain fermentable sugars. J Chem. https://doi.org/10.1155/2017/5680105

Asad M, Saba N, Asiri AM, Jawaid M, Indarti E, Wanrosli WD (2018) Preparation and characterization of nanocomposite films from oil palm pulp nanocellulose/poly (Vinyl alcohol) by casting method. Carbohyd Polym 191:103–111. https://doi.org/10.1016/j.carbpol.2018.03.015

Asaeda T, Rajapakse L, Manatunge J, Sahara N (2006) The effect of summer harvesting of *phragmites australis* on growth characteristics and rhizome resource storage. Hydrobiologia 553:327–335. https://doi.org/10.1007/s10750-005-6

Baghban MH, Mahjoub R (2020) Natural Kenaf fiber and LC3 binder for sustainable fiber-reinforced cementitious composite: a review. Appl Sci 357:1–15. https://doi.org/10.3390/app10010357

Banerjee M, Saraswatula S, Williams A, Brettmann B (2020) Effect of purification methods on commerciallyavailable cellulose nanocrystal properties andTEMPO oxidation. Processes 8:698. https://doi.org/10.3390/pr8060698

Barbash V, Yaschenko O (2020) Preparation, properties and use of nanocellulose from non-wood plant materials. In: Krishnamoorthy K (ed) Novel nanomaterials. IntechOpen, London

Barbash VA, Yaschenko OV, Alushkin SV, Kondratyuk AS, Posudievsky OY, Koshechko VG (2016) The effect of mechanochemicaltreatment of cellulose on characteristics of nanocellulosefilms. Nanoscale Res Lett 11:410. https://doi.org/10.1186/s11671-016-1632-1

Barbash VA, Yaschenko OV, Shniruk OM (2017a) Preparation andproperties of nanocellulose from organosolv straw pulp. Nanoscale Res Lett 12:241. https://doi.org/10.1186/s11671-017-2001-4

Barbash V, Yashchenko O, Kedrovska A (2017b) Preparation and propertiesof nanocellulose from peracetic flax pulp. JSRR 16(1):1–10. https://doi.org/10.9734/JSRR/2017/36571

Barbash VA, Yashchenko OV, Opolsky VO (2018) Effect of hydrolysis conditions of organosolv pulp from kenaf fibers on the physicochemical properties of the obtained nanocellulose. Theor Exp Chem 54:193–198. https://doi.org/10.1007/s11237-018-9561-y

Barbash VA, Yashchenko OV, Vasylieva OA (2019) Preparation and properties of nanocellulose from miscanthus × giganteus. J Nanomater. https://doi.org/10.1155/2019/3241968

Besbes I, Alilsa S, Boufi S (2011) Nanofibrillated cellulose from TEMPO-oxidizede ucalyptus fibres:effect of the carboxyl content. Carbohydr Polym 84(3):975–983

Biana H, Gaoa Y, Yanga Y, Fang G, Daia H (2018) Improving cellulose nanofibrillation of waste wheat straw using the combined methods of prewashing, *p*-toluenesulfonic acid hydrolysis, disk grinding, and endoglucanase post-treatment. Biores Technol 256:321–327. https://doi.org/10.1016/j.biortech.2018.02.038

Charani PR, Moradian MH (2019) Utilization of cellulose nanofibers and cationic polymers to improve breaking length of paper. Cellul Chem Technol 53(7–8):767–774

Chen Y, Fan D, Han Y, Lyu S, Lu Y, Li G, Jiang F, Wang S (2018) Effect of high residual lignin on the properties f cellulose nanofibrils/films. Cellulose 25:6421–6431. https://doi.org/10.1007/s10570-018-2006-x

Choi JH, Park SY, Kim JH, Cho SM, Jang SK, Hong C, Choi IG (2019) Selective deconstruction of hemicellulose and lignin with producing derivatives by sequential pretreatment process for biorefining

concept. Bioresour Technol 291:121913. https://doi.org/10.1016/j.biortech.2019.121913
Coseri S (2009) Phthalimide-*N*-oxyl (PINO) radical, a powerful catalytic agent: its generation and versatility towards various organic substrates. Catal Rev 51(2):218–292. https://doi.org/10.1080/01614940902743841
Dassanayake RS, Acharya S, Abidi N (2018) Biopolymer-based materials from polysaccharides: properties processing, characterization and sorption applications. In: Edebali S (ed) Advanced sorption process applications. IntechOpen, London
Deykun I, Halysh V, Barbash V (2018) Rapeseed straw as an alternative for pulping and papermaking. Cellulose Chem Technol 52(9–10):833–839
Dias OAT, Konar S, Leão AL, Yang W, Tjong J, Sain M (2020) Current stateof applications of nanocellulose in flexible energy and electronic devices. Front Chem. https://doi.org/10.3389/fchem.2020.00420
Esmaeil MHK, Talaeipour M, Bazyar B, Mirshokraei SA, Eslam HK (2019) Two-step delignification of peracetic acid and alkali from sugar cane bagasse. BioResources 14(4):9994–10003
Feng X, Zhao Y, Jiang Y, Miao M, Cao S, Fang J (2017) Use of carbon dots to enhance UV-blocking of transparent nanocellulose films. Carbohyd Polym 161:253–260. https://doi.org/10.1016/j.carbpol.2017.01.030
Gopakumar DA, Arumughan V, Pasquini D, Leu B, Thomas S (2019) Nanocellulose-based membranes for water purification. Nanoscale Mater Water Purif. https://doi.org/10.1016/b978-0-12-813926-4.00004-5
Hirota M, Tamura N, Saito T, Isogai A (2010) Water dispersion of cellulose II nanocrystals prepared by TEMPO mediated-oxidation of mercerized cellulose at pH 4.8. Cellulose 17:279–288
Ilyas RA, Sapuan SM, Ishak MR, Zainudin ES (2017) Effect of delignification on the physical, thermal, chemical, and structural properties of sugar palm fibre. BioResources 12(4):8734–8754
Isogai A (2018) Development of completely dispersed cellulose nanofibers. Proc Jpn Acad Ser B 94:161–178. https://doi.org/10.2183/pjab.94.012
Jahan MS, Rumee JN, Rahman MM, Quaiyyum A (2014) Formic acid/acetic acid/water pulping of agricultural wastes. Cellul Chem Technol 48(1–2):111–118
Jambeck JR, Andrady A, Geyer R, Narayan R, Perryman M, Siegler T, Wilcox C, Lavender LK (2015) Plastic wasteinputs from land into the ocean. Science 347:768–771
Jasmani L, Thielemans W (2018) Preparation of nanocellulose and its potential application. For Res 7:1–8. https://doi.org/10.4172/2168-9776.1000222
Kargarzadeh H, Ioelovich M, Ahmad I, Thomas S, Dufresne A (2017) Methods for extraction of nanocellulosefrom various sources. In: Kargarzadeh H, Ioelovich M, Ahmad I, Thomas S, Dufresne A (eds) Handbook of nanocellulose and cellulosenanocomposites. Wiley, Weinheim, pp 1–49
Klemm D, Heublein B, Fink H-P, Boh A (2005) Cellulose: fascinating biopolymer and sustainable raw material. Angew Chem Int Ed 44:3358–3393. https://doi.org/10.1002/anie.200460587
Kumar R, Huc F, Hubbell CA, Ragauskas AJ, Wyman CE (2013) Comparison of laboratory delignification methods, their selectivity, and impacts on physiochemical characteristics of cellulosic biomass. Biores Technol 130:372–381. https://doi.org/10.1016/j.biortech.2012.12.028
Levanič J, Šenk VP, Nadrah P, Poljanšek I, Oven P, Haapala A (2020) Analyzing TEMPO-oxidized cellulose fiber morphology: new insights into optimization of the oxidation process and nanocellulose dispersion quality. ACS Sustain Chem Eng 8(48):17752–17762. https://doi.org/10.1021/acssuschemeng.0c05989
Long L, Tian D, Hu J, Wang F, Saddler J (2017) A xylanase-aided enzymatic pretreatment facilitates cellulose nanofibrillation. Bioresour Technol 243:898–904. https://doi.org/10.1016/j.biortech.2017.07.037
Lu P, Liu R, Liu X, Wu M (2018) Preparation of self-supporting bagasse cellulose nanofibrils hydrogels induced by zinc ions. Nanomaterials 8:800. https://doi.org/10.3390/nano8100800
Madivoli ES, Kareru PG, Gachanja AN, Mugo SM, Sujee DM, Fromm KM (2020) Isolation of cellulose nanofibers from oryzasativa residues via tempo mediated oxidation. J Nat Fibers. https://doi.org/10.1080/15440478.2020.1764454
Mahmud MM, Asma M, Asma P, Perveen A, Jahan RA, Arafat MT (2019) Preparation of different polymorphs of cellulose from different acid hydrolysis medium. Int J Biol Macromol. https://doi.org/10.1016/j.ijbiomac.2019.03.027
Milanovich J, Kostic M, Skundric P (2012) Strucrure and properties of TEMPO-oxidized cotton fibers. Chem Ind Chem Eng Q 18(3):473–481
Naz S, Ali JS, Zia M (2019) Nanocellulose isolation characterization and applications: a journey from non-remedial to biomedical claims. Bio-Des Manuf. https://doi.org/10.1007/s42242-019-00049-4
Paschoal G, Muller CM, Carvalho GM, Tischera CA, Malia S (2015) Isolation and characterization of nanofibrillated cellulose from oat hulls. Quim Nova 38(4):478–482. https://doi.org/10.5935/0100-4042.20150029
Patiño-Masó J, Serra-Parareda F, Tarrés Q, Mutjé P, Espinach FX, Delgado-Aguilar M (2019) TEMPO-oxidized cellulose nanofibers: a potential bio-based superabsorbent for diaper production. Nanomaterials 9:1271. https://doi.org/10.3390/nano9091271
Phanthong P, Reubroycharoen P, Hao X, Xu G, Abudula G, Guan G (2018) Nanocellulose: extraction and application. Carbon Resour Convers 1:32–44
Plermjai K, Boonyarattanakalin K, Mekprasart W, Pavasupree S, Phoohinkong W, Pecharapa W (2010) Extraction and characterization of nanocellulose from sugarcane bagasse by ball-milling-assisted acid hydrolysis. AIP Conf Proc. https://doi.org/10.1063/1.5053181
Rol F, Belgacem MN, Gandini A, Bras J (2019) Recent advances in surfacemodified cellulose nanofibrils. Prog Polym Sci 88:241–264. https://doi.org/10.1016/j.progpolymsci.2018.09.002
Saberikhan E, Rovsseh JM, Rezayati-Charani P (2011) Organosolv pulping of wheat straw by glycerol. Cellul Chem Technol 45(1–2):67–75
Saltonstall K (2002) Cryptic invasion by a non-native genotype of thecommon reed, *phragmites australis*, into North America. PNAS 99(4):2445–2449. https://doi.org/10.1073/pnas.032477999
De Santi V, Cardellini F, Brinchi L, Germani R (2012) Novel bronsted acidic deep eutectic solvents as reaction media for esterification of carboxylic acid with alcohols. Tetrahedron Lett 53(38):5151–5155
Sánchez R, Espinosaa E, Domínguez-Roblesa J, Mauricio Loaiza J, Rodrígueza A (2016) Isolation and characterization of lignocellulose nanofibers from different wheat straw pulps. Int J Biol Macromol 92:1025–1033. https://doi.org/10.1016/j.ijbiomac.2016.08.019
Schmidt C, Krauth T, Wagner S (2017) Export of plastic debris by rivers into the sea. Environ Sci Technol 51(21):12246–12253 (**Bibcode:2017EnST...5112246S**)
Segal LC, Creely JJr, Martin AEJ, Conrad CM (1959) An empirical method for estimating the degree of crystallinity of native cellulose using the X-ray diffractometer. Text Res J 29(10):786–794. https://doi.org/10.1177/004051755902901003
Seta FT, Ana X, Liua L, Zhanga H, Yanga J, Zhanga W (2020) Preparation and characterization of high yield cellulose nanocrystals (CNC) derived from ball mill pretreatment and maleic acid hydrolysis. Carbohyd Polym 234:115942. https://doi.org/10.1016/j.carbpol.2020.115942

Shaghaleh H, Xu X, Wang S (2018) Current progress in production of biopolymeric materials based on cellulose, cellulose nanofibers, and cellulose derivatives. RSC Adv 8:825–842. https://doi.org/10.1039/C7RA11157F

Shak KPY, Pang YL, Mah SK (2018) Nanocellulose: recent advances and its prospects in environmental remediation. Beilstein J Nanotechnol 9:2479–2498. https://doi.org/10.3762/bjnano.9.232

Sharma A, Thakur M, Bhattacharya M, Mandal T, Goswamia S (2019) Commercial application of cellulose nano-composites—a review. Biotechnol Rep. https://doi.org/10.1016/j.btre.2019.e00316

Sosiati H, Wijayanti DA, Triyana K, Kamiel B (2017) Morphology and crystallinity of sisal nanocellulose after sonication. AIP Conf Proc 1877:030003–1-030003–7

Sun X, Wu Q, Ren S, Lei T (2015) Comparison of highly transparent all-cellulose nanopaper prepared using sulfuric acid and TEMPO-mediated oxidation methods. Cellulose 22(2):1123–1133. https://doi.org/10.1007/s10570-015-0574-6

Thomas B, Raj MC, Athira KB, Rubiyah MH, Joy J, Moores A, Drisko GL, Sanchez C (2018) Nanocellulose, a versatile green platform: from biosources to materials and their applications. Chem Rev 118(24):11575–11625. https://doi.org/10.1021/acs.chemrev.7b00627

Torlopov MA, Mikhaylov VI, Udoratina EV, Aleshina LA, Prusskii AI, Tsvetkov NV, Krivoshapkin PV (2017) Cellulose nanocrystals with different length-to-diameter ratios extracted from various plants using novel system acetic acid/phosphotungstic acid/octanol-1. Cellulose 25(2):1031–1046. https://doi.org/10.1007/s10570-017-1624-z

Trache D, Tarchoun AF, Derradji M, Hamidon TS, Masruchin N, Brosse N, Hussin MH (2020) Nanocellulose: from fundamentals to advanced applications. Front Chem 8:392. https://doi.org/10.3389/fchem.2020.00392

Vurasko AV, Glukhikh VV, Simonova EI, Minakova AR (2018) Statistic simulation of the delignification process. In: Proceedings of the annual scientific international conference Nizhniy Tagil, Russia, 4 May 2018, pp 7–16

Yang Y, Chen Z, Zhang J, Wang G, Zhang R, Suo D (2019) Preparation and applications of the cellulose nanocrystals. Int J Polym Sci. https://doi.org/10.1155/2019/1767028

Zhanga Y, Haoa N, Lina X, Niea S (2020) Emerging challenges in the thermal management of cellulose nanofibrilbased supercapacitors, lithium-ion batteries and solar cells: a review. Carbohyd Polym 234:115888. https://doi.org/10.1016/j.carbpol.2020.115888

Zhu H, Parvinian S, Preston C, Vaaland O, Ruan Z, Hu L (2013) Transparent nanopaper with tailored optical properties. Nanoscale 5:3787–3792